The influence of various mineral admixtures on the shrinkage behavior of shotcrete

Bofang Zhang and Zhenbo Wang
School of Mechanics and Civil Engineering, China University of Mining and Technology – Beijing, Beijing, China

Received 24 October 2025
Revised 2 December 2025
Accepted 8 December 2025

Abstract

Purpose – The utilization of alkali-free accelerators, primarily based on aluminum sulfate, in shotcrete often leads to significant shrinkage and cracking, jeopardizing long-term durability. This study aims to mitigate this issue by investigating the efficacy of silica fume (SF) and fly ash (FA), individually and combined, in controlling the shrinkage deformation of shotcrete.

Design/methodology/approach – Shotcrete mixtures were prepared with cement partially replaced by SF, FA, or their combination (SF-FA). Aluminum sulfate was used as an accelerator. The shrinkage behavior under sealed and dry conditions was monitored. The underlying mechanisms were elucidated through hardened air-void analysis, mercury intrusion porosimetry (MIP), and internal humidity tracking.

Findings – Contrary to some previous studies, both individual and combined incorporation of mineral admixtures reduced the 28-day shrinkage. The SF-FA composite exhibited the most substantial reduction (23.72% sealed, 17.76% dry), followed by SF alone (18.11% sealed) and FA alone (11.35% sealed). Mechanism analysis revealed that the admixtures refined the pore structure, reduced the volume of harmful pores, and, crucially, optimized the air-void system by increasing the population of fine bubbles. This created an internal buffering effect that alleviates capillary stress. The synergistic effect in the SF-FA group is attributed to complementary pore-filling at dual scales.

Originality/value – This work demonstrates that, within an aluminum sulfate-accelerated shotcrete system, silica fume can effectively reduce shrinkage when its pore-refining effect is counterbalanced by a well-optimized micro-bubble network. It provides the first comprehensive evidence of the synergistic shrinkage-reducing mechanism of SF and FA in such systems, offering a practical strategy for mix design optimization to enhance the volume stability of shotcrete.

Keywords Shotcrete, Alkali-free accelerator, Mineral admixtures, Shrinkage, Pore structure

Paper type Research article

1. Introduction

Shotcrete, a specialized form of concrete applied by spraying, is a crucial material in the construction industry, particularly in infrastructure projects like highways, railways, and water management systems (Li, Zhang, Niu, & Song, 2020). Its unique application method, which eliminates the need for formwork, makes it a preferred choice for various construction scenarios. In tunnel construction for transportation networks, shotcrete plays a pivotal role in providing initial structural support. This is essential for managing rock deformation after blasting, preventing collapses, and ensuring the safety of both workers and equipment within the tunnel environment. Accelerators are often added to shotcrete mixtures to expedite the setting process and enhance early strength development (Tang, Xu, Lian, & Qu, 2016; Garba *et al.*, 2024; Yang, He, & Xu, 2022). However, the use of accelerators has caused a series of durability problems in shotcrete, among which the cracking phenomenon caused by shrinkage deformation is particularly prominent.

Railway Sciences
Vol. 5 No. 1, 2026
pp. 49-66
Emerald Publishing Limited
e-ISSN: 2755-0915
p-ISSN: 2755-0907
DOI 10.1108/RS-10-2025-0049

Accelerators are generally classified into alkaline accelerators and alkali-free accelerators based on their alkali content. The alkali content of alkali-free accelerators is less than 1%, while that of alkaline accelerators is higher than 1% (British Standards Institution, 2005). Currently, alkali-free accelerators with aluminum sulfate as the main component are gradually replacing alkaline accelerators due to their low alkali content, safety, environmental friendliness, rapid setting, and minimal impact on concrete strength (Prudencio, 1998). However, the use of alkali-free accelerators significantly impairs the durability of shotcrete, particularly manifested as cracking caused by shrinkage deformation. Austin and Robins (E&FN Spon, 1995) compared the shrinkage behavior of shotcrete and traditional concrete and found that the total shrinkage rate of shotcrete was significantly higher. Wang, Li, and Tan (2023) observed that both the autogenous shrinkage and drying shrinkage of shotcrete increased significantly under the action of alkali-free accelerators. Sheng, Xue, and Li (2017) developed an alkali-free liquid accelerator based on aluminum sulfate and conducted studies on three dosage levels (5%, 7%, and 9%). The results showed that the dosage of the accelerator was directly related to the shrinkage strain of shotcrete - the higher the dosage, the greater the shrinkage rate. Huang (2021) pointed out that the alkali-free accelerator composed of aluminum sulfate and fluoroaluminate complex accelerated the early shrinkage rate of cement paste; however, the shrinkage rate slowed down over time, and at the same age, the paste shrinkage rate decreased with the increase in accelerator dosage. Given that aluminum sulfate is the core active component for accelerating setting and early strength development of alkali-free accelerators and its composition system is relatively complex, aluminum sulfate was used to replace the alkali-free accelerator in this study.

In the past shrinkage inhibition research, silica fume (SF), fly ash (FA) and other mineral admixtures have been widely used in ordinary concrete. When it is used in shotcrete, it can not only improve the utilization rate of solid waste, reduce carbon emission, but also improve workability and durability. However, research on controlling the shrinkage of sprayed concrete with admixtures is still limited. Bruce, Alexandre, and Marc (2022) found that FA reduces rebound, increases porosity, and reduces total shrinkage in dry-mix shotcrete. Wan, He, and Zheng (2024). studied the effect of SF/FA on alkali-free accelerator modified mortar, pointing out that SF can improve early strength and durability, but will significantly increase shrinkage; FA can improve volume stability, but high content will accelerate the internal humidity decline. Li (2013) obtained through the test, the results show that: FA admixture can significantly reduce the early self-shrinkage of high performance concrete, while SF will increase its early self-shrinkage; at the same time, the impact of ground slag on self-shrinkage is related to its fineness and content. However, some scholars have found different experimental phenomena. Wang, Zeng, and Qiao (2022a) found that FA and slag powder single or compound admixture in low content conditions will cause further deterioration of the drying shrinkage performance of shotcrete, in which the deterioration caused by FA is greater than slag powder. Currently, the shrinkage deformation of cement-based materials is often described as a two-stage process: rapid chemical shrinkage during the early humidity-saturated stage, and subsequent shrinkage deformation induced by self-desiccation or drying during the humidity-declining stage (Zhang, Hou, & Wei, 2010; Wang *et al.*, 2023). The shrinkage deformation of cement-based materials is closely related to the evolution of internal relative humidity (Zhang, Hou, & Han, 2012). This pattern provides a foundation for analyzing the shrinkage mechanisms of cement-based materials. However, in the complex system of shotcrete containing aluminum sulfate-based accelerators, how mineral admixtures affect the progression and magnitude of these two stages, and their underlying micro-mechanisms, have not yet been systematically elucidated.

While most of the aforementioned studies have focused on the drying shrinkage or autogenous shrinkage of shotcrete, with limited research addressing the simultaneous control of both shrinkage types. Moreover, the majority of existing studies employ a single addition of mineral admixtures and have not systematically compared the effects of single versus combined additions on the shrinkage deformation of shotcrete. This paper selects SF and FA as the primary research materials. By partially replacing cement using both single and compound blending methods, it investigates the synergistic regulatory effects of SF and FA on the autogenous shrinkage and drying shrinkage of shotcrete, elucidating their influence on shrinkage deformation. Additionally, through an analysis of pore structure parameters in hardened concrete and mercury intrusion porosimetry tests, the internal mechanisms by which mineral admixtures affect the shrinkage deformation of shotcrete are clarified at the microscopic level. Finally, an optimized application scheme for mineral admixtures that effectively controls the shrinkage deformation of shotcrete is proposed.

2. Experiments and materials

2.1 Raw materials

The raw materials used in the shotcrete test in this study are as follows: The cement was Ordinary Portland Cement (P.O 42.5) produced by Beijing Jinyu Group Co., Ltd. Its chemical composition and mineral constituents are provided in Table 1, with its particle size distribution shown in Figure 1. The fine aggregate was medium sand with a fineness modulus of 2.94 and an apparent density of 2,423 kg/m^3. The coarse aggregate was crushed stone with a particle size range of 5–10 mm and an apparent density of 2,783 kg/m^3. The mineral admixtures included Grade I low-calcium fly ash and SF-90 grade silica fume produced by Gansu Sanyuan Silicon Materials Co., Ltd. To ensure adequate workability of the concrete, a polycarboxylate superplasticizer was incorporated. The accelerator used was analytically pure aluminum sulfate octadecahydrate ($Al_2(SO_4)_3 \cdot 18H_2O$) supplied by Sinopharm Chemical Reagent Co., Ltd.

2.2 Experimental mix proportions

To investigate the impact of different admixtures on shotcrete shrinkage, four shotcrete series were analyzed: a control group, FA only, SF only, and a combination of SF and FA, labeled JZ, FA, SF, and SF-FA, respectively. The mixture ratios are detailed in Table 2.

The experiment utilized the mixing ratios specified in Table 2. The blank control group was denoted as JZ. FA comprised 15% of the total cementitious material by mass, while SF made up 5% of the cementitious material by mass. A combination of FA and SF, denoted as SF-FA, accounted for 15% of the cementitious material by mass. The aluminum sulfate was applied at a rate of 4% of the gelling material by mass, and the superplasticizer at 0.9% of the gelling material by mass.

Table 1. Chemical composition and main mineral composition of cement

Chemical composition		Main mineral composition	
Component	Content (%)	Component	Content (%)
SiO_2	18.89	C_3S	50.57
Al_2O_3	6.41	C_2S	16.01
Fe_2O_3	3.19	C_4AF	9.71
CaO	62.80	C_3A	12.97
Na_2O	0.36	$CaSO_4$	6.17
K_2O	0.86		
MgO	2.62		
SO_3	3.63		
LOI	/		

Source(s): Authors' own work

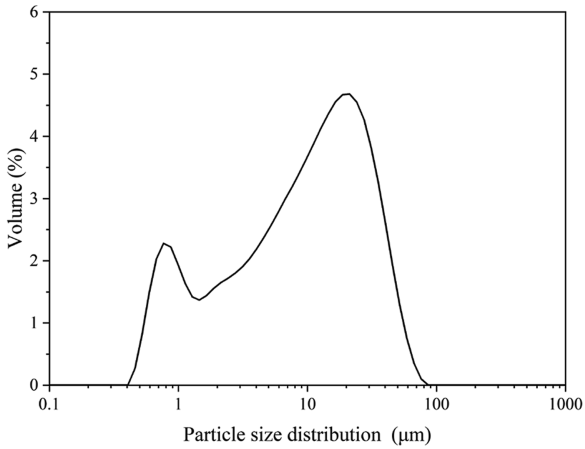

Figure 1. Cement particle size distribution. Source: Authors' own work

Table 2. Mix proportion of shotcrete test

Num	Materials (kg/m^3) Cement	Sand	Stone	Water	FA	SF	Aluminum sulfate	Superplasticizer
JZ	470	850	850	175			4%	0.9%
FA	399.5	850	850	175	70.5		4%	0.9%
SF	446.5	850	850	175		23.5	4%	0.9%
SF-FA	376	850	850	175	70.5	23.5	4%	0.9%

Source(s): Authors' own work

2.3 Method

2.3.1 Performance evaluation. The mechanical strength of shotcrete will be evaluated according to the "Standard for test methods of physical and mechanical properties of concrete" (GB/T 50,081–2019). To test the influence law of mineral admixtures on the compressive strength of shotcrete, 12 cube specimens with dimensions of 100 × 100 × 100 mm will be prepared for each test mix proportion. After molding, the specimens will be cured in a standard curing chamber. The compressive strength will be measured using a WAW-600Q pressure testing machine at the corresponding ages (3, 7, 14, and 28 d) to monitor the strength development law.

2.3.2 Shrinkage and humidity integration test of shotcrete. A linear variable differential transformer (LVDT) was employed to measure the shrinkage deformation of shotcrete, with a measuring range of 2 mm and an accuracy of 1μm. The LVDT was coaxially positioned to accurately capture the deformation of the shotcrete material over time. The shrinkage specimens were molded in a special plexiglass mold with an inner diameter of 400 × 100 × 100 mm, and extractable thin plates were arranged around the mold (Hou, 2010). Before the initial setting of the specimens, the thin plates around the mold were pulled out to allow the specimens to deform freely, and each specimen was sealed with butter and plastic film. Finally, a magnetic device was used to fix the LVDT at both ends of the specimens to determine the free shrinkage deformation law of the specimens. In addition to the LVDT, a capacitive sensor was also installed in the experimental device to monitor the temperature and humidity changes at a depth of 5 cm below the sample interface. This depth corresponds to the geometric center of the specimen, effectively minimizing direct interference from rapid surface drying and boundary effects, thereby allowing it to sensitively reflect the overall trend and rate of moisture migration from the interior outward. The sensor was placed in a PVC pipe for auxiliary positioning, and two rectangular holes with a width of 2 mm were opened on both sides of the bottom of the PVC pipe to ensure the moisture exchange between the sensor and the shotcrete around the holes. The humidity measuring range of the sensor was 0% to 100%, with an accuracy of 1%. Before conducting the experiment, the capacitive sensor underwent a calibration procedure using distilled water and standard saturated salt solutions under controlled temperature conditions. Then, the obtained calibration curve (see Figure 2) was applied to adjust the humidity data obtained from the shotcrete specimens to ensure the accuracy and reliability of the collected data. Table 3 presents the theoretical humidity values of distilled water and various standard saturated salt solutions, which serve as reference points for calibrating and verifying the humidity sensor readings during the experimental measurement.

For the shrinkage and humidity tests of shotcrete, two parallel specimens are formed for each mix ratio, namely the dry specimen and the sealed specimen. After sealing, all specimens and data acquisition equipment were placed in a laboratory maintained at 16 ± 1°C and 60 ± 5% RH. The shrinkage deformation and internal humidity development of the specimens under sealed drying conditions were continuously measured to ensure comparability of the results. In the first 3 days of the test, both the sealed and dry specimens are kept sealed with plastic film. After 3 days, remove the plastic sealing film on the top and around the dry specimen to allow it to fully contact the external environment, while the sealed specimen remains unchanged until the end of the test, as shown in Figure 3.

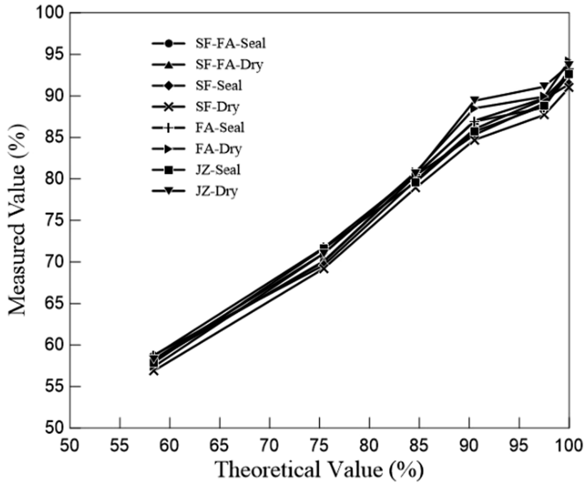

Figure 2. Humidity sensor calibration curve. Source: Authors' own work

Table 3. Theoretical humidity values of distilled water and saturated salt solution

Saturated salt solution	NaBr	NaCl	KCl	$BaCl_2$	K_2SO_4	Distilled water
Theoretical humidity/%	58.4	75.4	84.6	90.5	97.5	100

Source(s): Authors' own work

Figure 3. Shrinkage and humidity test specimens. Source(s): Authors' own work

2.3.3 Concrete bubble parameter analysis. The research utilizes a digital bubble spacing coefficient tester to analyze the bubble properties in shotcrete. The test samples consist of 100 mm cubic specimens that undergo a 28 d curing process before being sliced into 100 mm × 100 mm × 10 mm sections. These sections are meticulously polished to attain a surface roughness not exceeding $Ra \leq 0.1 \mu m$. Subsequently, an optical microscope is employed to examine the polished sections, enabling the measurement of bubble chord length and spacing along a specified scan line. For each mixture ratio, three slices are meticulously prepared, and the average measurements from these slices are aggregated to determine the final outcomes for each test cohort.

2.3.4 Pore structure analysis. The mercury intrusion test, a common method for evaluating pore structures, was employed to analyze the specimen. To provide a detailed representation of the internal pore structure of shotcrete, cement paste obtained from the 28d strength test was utilized for sample preparation. Subsequently, these samples underwent a 24-h immersion in absolute ethanol followed by drying in a vacuum oven until reaching a consistent weight. The pore size distribution analysis was carried out using the Micromeritics AutoPore IV 962, which covered a broad range from 0.003 to 450 µm.

3. Results and discussion

3.1 Compressive strength

Figure 4 illustrates the compressive strength test outcomes for four distinct mixtures at varying ages. A comparison between the JZ group and the FA group shows that the FA group showed a notable increase of 1.4% and 5.6% in compressive strength at 14 and 28 days, respectively. Similarly, the SF group exhibited enhancements of 5.7% and 8.8% in compressive strength at 14 and 28 days, while the SF-FA group displayed improvements of 3.6% and 9.7% at the same time points. It is important to note that the ranking of 3-day compressive strength across the groups was SF > JZ > SF-FA > FA. The effectiveness of mineral admixtures, such as SF and FA, in improving shotcrete strength can be attributed to their fine particle sizes. These admixtures utilize a micro-aggregate effect to penetrate the pores of the cement paste, leading to the densification of the concrete structure. Silica fume, with its SiO_2 content, and FA, containing Al_2O_3, engage in a pozzolanic reaction with calcium hydroxide (CH) produced

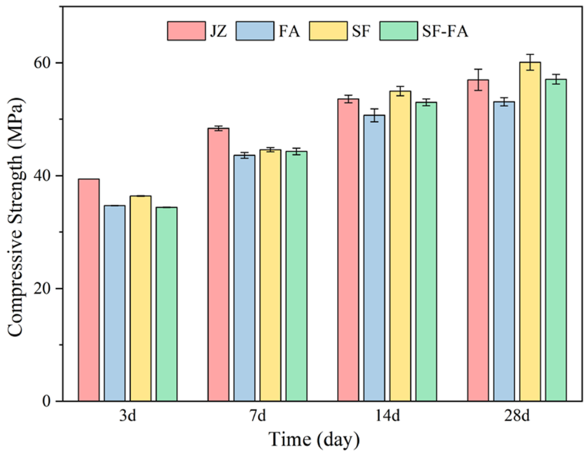

Figure 4. Compressive strength curves of shotcrete at different age. Source(s): Authors' own work

during cement hydration. This reaction results in the formation of a significant amount of Calcium Silicate Hydrate gel (C-S-H), which fills the voids in the cement paste and enhances the strength of the concrete. Partially replacing cement with FA affects the early hydration process of cement. The active Al_2O_3 in fly ash gradually dissolves, increasing the concentration of Al^{3+} in the solution, breaking the hydration equilibrium of C_3A, and leading to the massive formation of expansive ettringite, which in turn causes a decrease in the strength of shotcrete (Wang, He, Shu, Wei, & Wang, 2022b). In addition, the difference in reactivity between fly ash and silica fume leads to a delayed reaction of fly ash, resulting in slow strength development of specimens in the FA group. Therefore, although the 3d compressive strength of the JZ group is higher than that of the SF-FA composite admixture group and the pure fly ash group, its strength improvement effect is inferior to that of the pure silica fume group (Qu, Yu, Ji, Gauvin, & Voets, 2020).

3.2 Shrinkage and internal humidity development analysis

This research conducted a comprehensive analysis of shrinkage deformation and internal humidity variations in specimens with four different mix proportions. The specimens were subjected to two distinct environmental conditions: sealed and dry. Two specimens were prepared for each mix proportion, allowing for comparative analysis between the sealed and dry environments. Detailed results and data are depicted in Figures 5–8.

According to the analysis of experimental results, regardless of being in a sealed or dry environment, the relative humidity (RH) of specimens in each group shows typical two-stage change characteristics with age (Han, Zhang, Wang, & Hao, 2017; Wang, Xie, Zhong, & Qu, 2022c). The first stage is the humidity saturation and stabilization period (RH ~ 100%). The reason for the stable humidity in this stage is that the hydration products (such as AFt and C-S-H) generated in the early stage of cement hydration adsorb a large amount of bound water, and the free water in the pores has not been significantly consumed; moreover, the dry specimens have not exchanged moisture with the environment. The second stage is the non-linear humidity attenuation period (after 3d). The humidity change in this stage is the result of the dynamic coupling effect of water consumption and migration. On the one hand, the continuous hydration of cement and the pozzolanic reaction of mineral admixtures will continuously consume free water. On the other hand, under the action of the micro-aggregate of mineral admixtures, the pore structure inside the shotcrete will evolve, affecting the water migration path, and then the humidity decline rate fluctuates non-linearly.

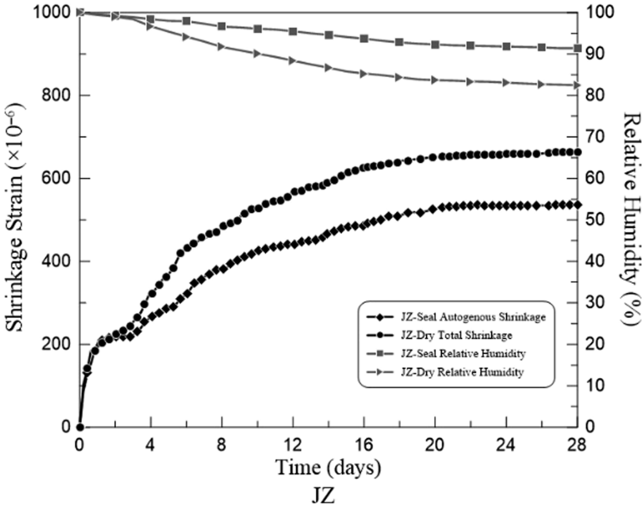

Figure 5. JZ shrinkage and humidity development curves. Source(s): Authors' own work

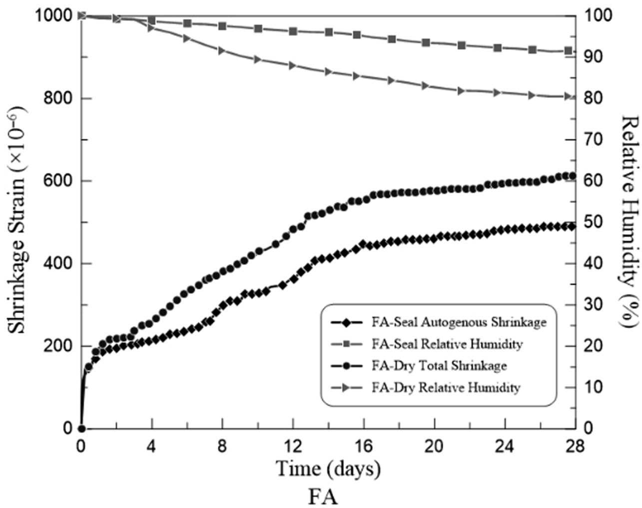

Figure 6. FA shrinkage and humidity development curves. Source(s): Authors' own work

In a sealed environment, humidity attenuation is entirely dominated by water consumption during the hydration process. The JZ group, without mineral admixtures, has a relatively higher cement content, leading to faster early hydration. This generates abundant hydration products such as ettringite and C-S-H, which rapidly consume free water within the system, resulting in a relatively high relative humidity attenuation rate in the specimen (Wang, Xie, Zhong, & Li, 2020). FA particles, with their spherical shape and smooth surface, exhibit a smaller specific surface area and lower pozzolanic reactivity (Wu, Farzadnia, Shi, Zhang, & Wang, 2017). Consequently, early water consumption in the specimen primarily derives from the sole hydration of cement. Meanwhile, as FA partially replaces cement, the absolute cement

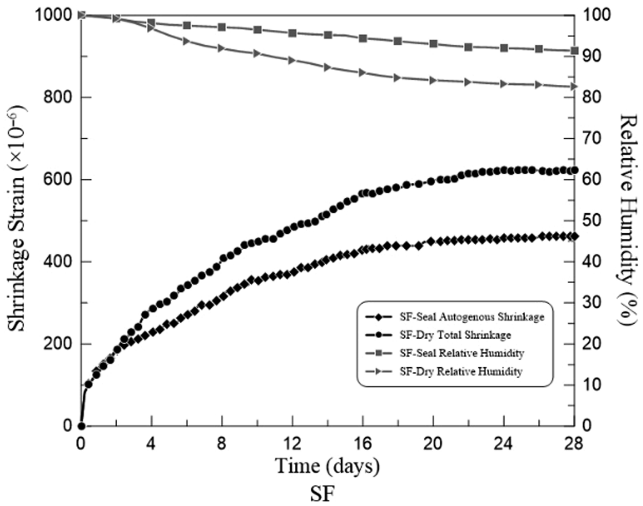

Figure 7. SF shrinkage and humidity development curves. Source(s): Authors' own work

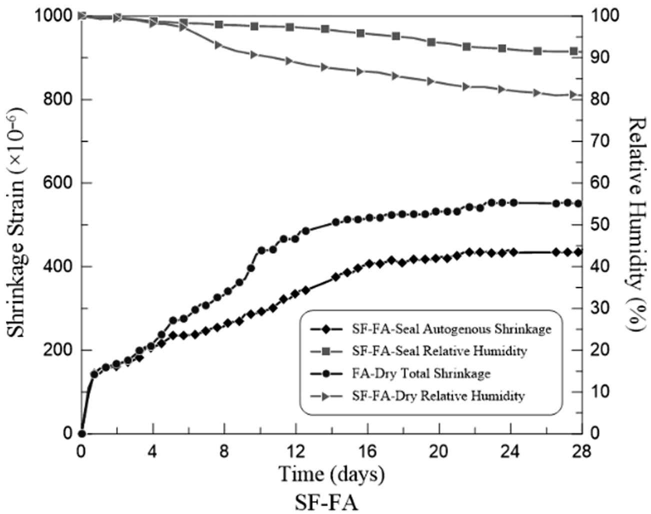

Figure 8. SF-FA shrinkage and humidity development curves. Source(s): Authors' own work

content in the system is lower than in the JZ group, significantly slowing the rate of free water consumption by cement hydration. Thus, the relative humidity attenuation rate in the FA group is slower than that of the JZ group. In the SF group, SF—characterized by its ultra-high specific surface area and submicron particle size (<0.1 μm)—exhibits an intense early pozzolanic reaction that accelerates cement hydration (Liu, Sun, Miao, 2009). This not only rapidly consumes a large amount of free water but also induces higher early hydration temperatures, making the humidity attenuation rate in the specimen the fastest. In a dry environment, humidity attenuation is driven by a combination of "hydration consumption + surface evaporation," accelerating humidity reduction across all groups.

Compared with the control group, the fine particles in the SF group fill pores, forming more developed evaporation channels within the specimen and causing humidity to decline more rapidly. FA particles, being spherical, retain free water more effectively than cement or SF particles, thereby delaying humidity attenuation. For the composite admixture group, building on the improved matrix compactness from pozzolanic reactions, SF fills gel pores (10–100 nm) while FA fills capillary pores (>100 nm). This “dual-scale filling” effect optimizes particle size grading, weakens pore connectivity, and further slows internal humidity decline, resulting in the lowest humidity attenuation rate.

The influence of mineral admixtures on the shrinkage deformation of shotcrete also shows two-stage characteristics: at the early age (0–4 d), the shrinkage deformation of each mix proportion increases rapidly at an approximately linear rate. Then, after the shrinkage reaches a certain value, the rate of shrinkage deformation increase begins to decelerate with the development of age. Among them, the rapid growth stage corresponds to the humidity saturation period, and the shrinkage in this stage is mainly related to the chemical shrinkage caused by cement hydration; the decelerating development stage corresponds to the humidity decline period, and the shrinkage deformation in this stage is mainly related to the self - drying caused by water migration and evaporation (Wang *et al.*, 2023). At 28d, the shrinkage values of the mineral admixture groups are all lower than those of the control group. Among them, the shrinkage of the sealed and dried specimens in the FA group is reduced by 11.35% and 8.53% respectively compared with the JZ group, that of the SF group is reduced by 18.11% and 6.76% respectively compared with the JZ group, and the SF - FA group shows the largest reduction, with the shrinkage of the sealed specimens decreased and that of the dried specimens decreased by 17.76%.

The above experimental results indicate that mineral admixtures can effectively inhibit the shrinkage of shotcrete, and the composite system of SF and FA exhibits a synergistic enhancement effect. The reason for the above differences lies in the synergistic regulation of the hydration process and microstructure by mineral admixtures: Firstly, the approximately spherical particles and low specific surface structure of FA can reduce the “squeezing effect” of water in the particle gaps, making it easier for free water to be retained in the pores of the paste, retaining more free water and delaying the formation of the internal humidity gradient, thereby improving the shrinkage deformation. In addition, the pozzolanic reaction of FA and SF undergoes a secondary reaction with CH, generating a large amount of C-S-H gel, which enhances the early stiffness and compactness of the matrix and inhibits the volume deformation of the specimen (Zhang, Zhang, & Yan, 2016). Secondly, the micro-aggregate effect of SF and FA synergistically optimizes the pore structure. They fill the internal pores, reducing the porosity and the proportion of connected pores, slowing down the water migration and evaporation rate (Li, Tan, & Zhang, 2000), and inhibiting the shrinkage deformation of the specimen. Finally, the composite system achieves shrinkage inhibition through hydration regulation: SF and FA replace part of the cement, weakening the intensity of the hydration reaction. Moreover, the hydration retardation of FA increases the effective water - binder ratio through the dilution effect, which is beneficial to reducing the early autogenous shrinkage of shotcrete.

3.3 Shotcrete bubble characteristics

Figures 9–14 depict the experimental results of the distribution of bubble diameter, average bubble diameter, and bubble spacing coefficient in hardened shotcrete. It can be observed from the figures that the bubble distribution in the JZ group exhibits the characteristics of “low frequency for small sizes and high sparsity for large sizes”, and the proportion of small bubbles (d < 50 μm) is relatively insufficient. After the incorporation of mineral admixtures, the size gradation of the bubble population is significantly improved: compared with the control group, the proportion of small bubbles in the FA group increases by 17.4%, that in the SF group increases by 14.3%, and the highest increase in the compound SF - FA group reaches 24.3%,

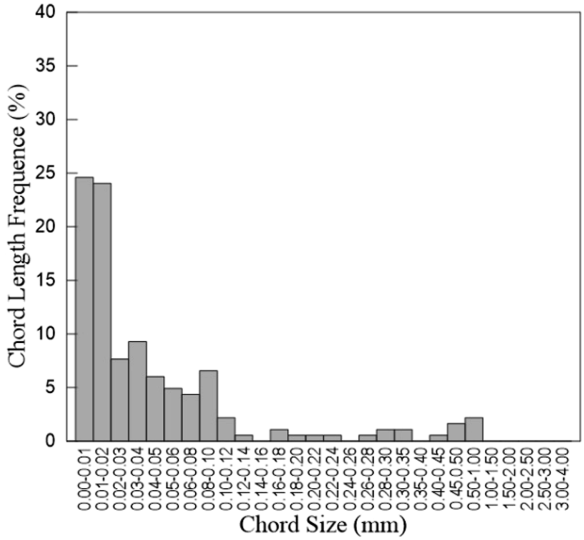

Figure 9. Hardened bubble pore size distribution of JZ. Source(s): Authors' own work

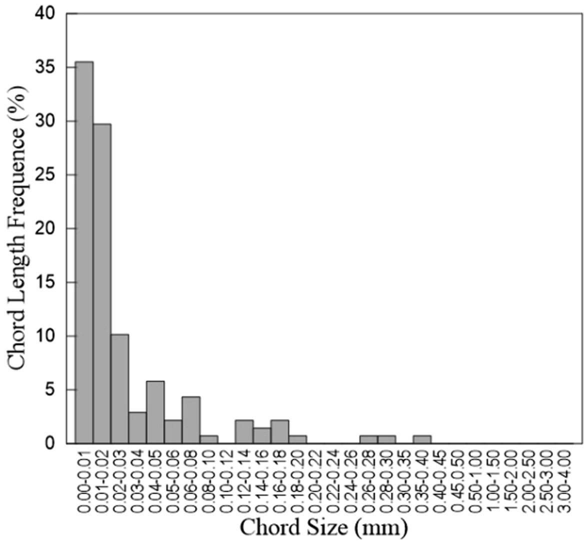

Figure 10. Hardened bubble pore size distribution of FA. Source(s): Authors' own work

indicating that mineral admixtures promote the formation of tiny bubbles and increase the number of "buffer units" in the matrix. The proportion of bubbles with a diameter of 50–100 μm shows a gradient decline trend with the addition of admixtures. Specifically, the FA group decreases by 54.3%, the SF group decreases by 44.7%, and the SF - FA group decreases by 35.9%. The number of large bubbles with a diameter >100 μm also decreases, with a 16.6% reduction in the SF group and an 11.2% reduction in the SF - FA group. In addition, mineral

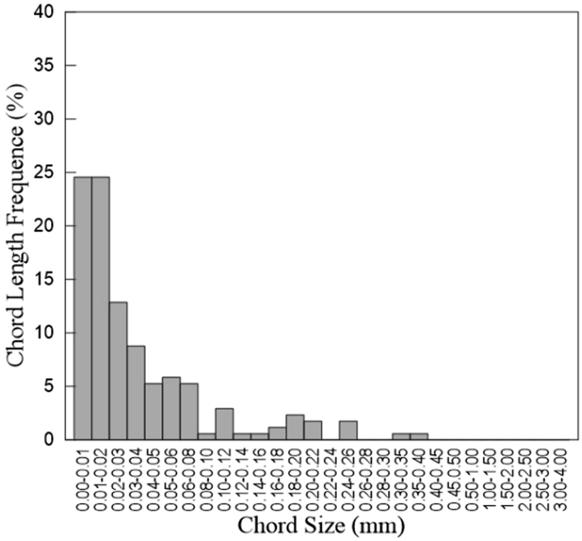

Figure 11. Hardened bubble pore size distribution of SF. Source(s): Authors’ own work

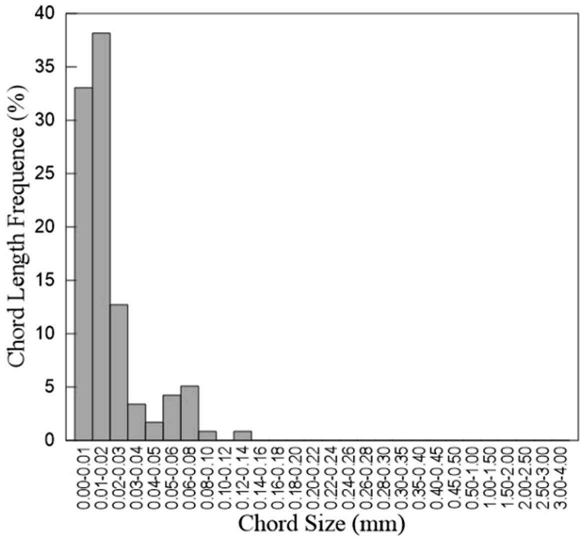

Figure 12. Hardened bubble pore size distribution of SF-FA. Source(s): Authors’ own work

admixtures shorten the bubble spacing coefficient, increase the density between bubbles, make the bubble distribution in the matrix more compact, and form an elastic buffer zone inside the specimen. As the relative humidity inside the specimen decreases, it can alleviate the shrinkage deformation of cement and other cementitious material particles caused by the increase in surface tension, and reduce the deformation driving force of the matrix (Hang, Sun, & Guo, 2020).

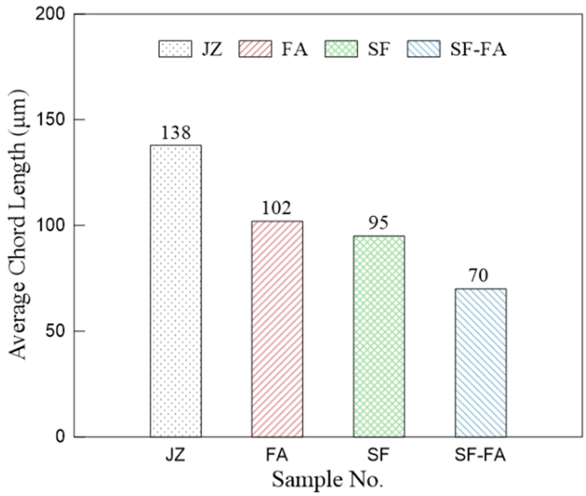

Figure 13. Average bubble diameter of shotcrete. Source(s): Authors' own work

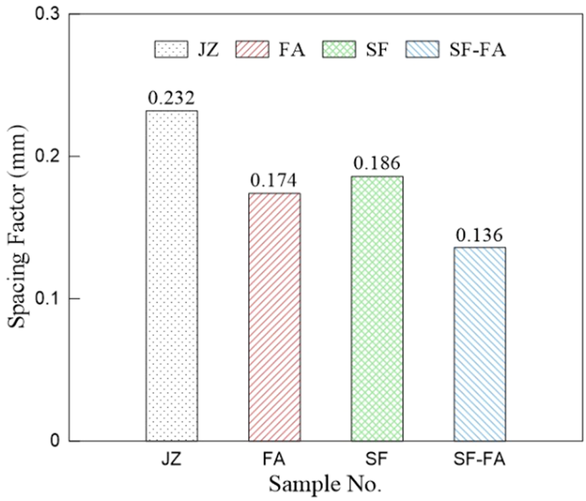

Figure 14. Shotcrete bubble spacing factor. Source(s): Authors' own work

3.4 Pore structure

The Mercury Intrusion Porosimetry (MIP) test is widely recognized as a fundamental technique for evaluating the pore characteristics of cementitious materials. These pores play a crucial role in determining capillary action, as well as the speed at which free water is absorbed and removed within the material. The pores present in cement paste are typically classified based on their size into four main categories: gel pores ($d \leq 10$ nm), medium capillary pores (10 nm $< d <$ 100 nm), large capillary pores (100 nm $\leq d \leq$ 1,000 nm), and air pores (($d \geq$ 1,000) (Deng, He, Lu, Wang, & Hu, 2023; Singh, Kumar, & Goyal, 2019; Yuan, Peng, & Li, 2021).

Figures 15–17 present the results of the MIP test, which indicate that mineral admixtures can quantitatively optimize the pore structure parameters. On the one hand, mineral admixtures significantly reduce the total porosity and total pore volume of shotcrete, and the effect of composite admixture is more remarkable. The total porosity of the control group at 28d is 15.23%, while that of the FA group decreases to 12.05%, the SF group to 9.85%, and the composite admixture group has the lowest porosity, which is 9.49%. On the other hand, it can be seen from Figure 16 that mineral admixtures change the internal pore size distribution of shotcrete. Under the action of admixtures, the overall volume fractions of gel pores and capillary pores inside the specimens of each group from large to small are as follows: JZ > SF > FA > SF-FA, which are 59.16%, 57.47%, 56.19%, and 53.08% respectively. The results of the SF and FA groups are similar, and the difference between the SF-FA group and the JZ group is the most significant.

The MIP test results reveal the microscopic mechanism by which mineral admixtures inhibit shrinkage through pore structure refinement. As shown in Figures 15–17, the incorporation of SF and FA, particularly in combination, significantly optimizes the pore structure parameters of shotcrete. On the one hand, mineral admixtures notably reduce the total

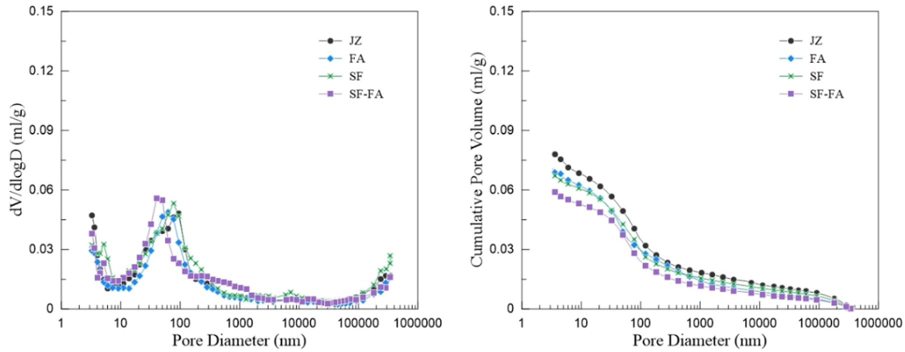

Figure 15. Differential curve and integral curve of shotcrete. Source(s): Authors’ own work

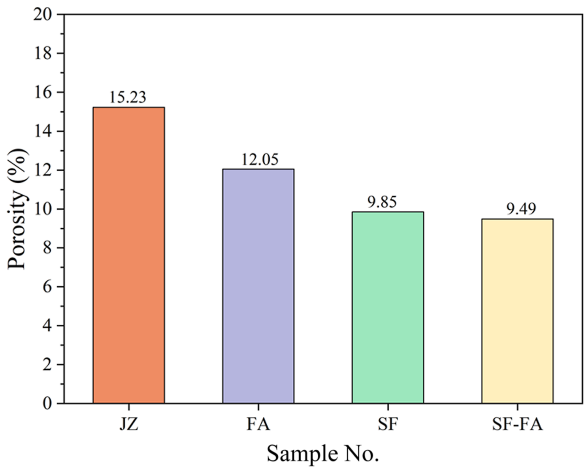

Figure 16. Specimen porosity. Source(s): Authors’ own work

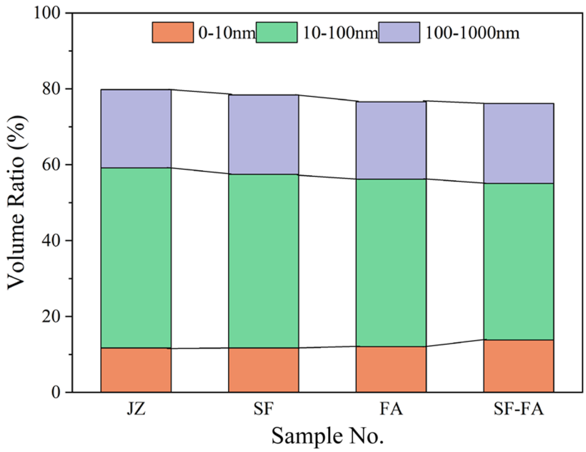

Figure 17. Pore volume fraction. Source(s): Authors' own work

porosity and total pore volume, with the group SF-FA exhibiting the most pronounced effect. The total porosity of the group JZ at 28 days was 15.23%, while that of the FA group, SF group, and SF-FA group decreased to 12.05%, 9.85%, and 9.49%, respectively. On the other hand, mineral admixtures alter the internal pore size distribution, leading to a reduction in the overall volume fractions of both gel pores and capillary pores.

According to the model proposed by Zhang *et al.* (2012), the shrinkage strain (ε_w) of cement-based materials depends simultaneously on its internal relative humidity (Ln(RH)) and pore structure characteristics (v_p), and can be expressed as the following functional relationship (Eq. 1). In the equation (1), the v_p is pore structure influence factor, whose physical meaning is the volume fraction of interconnected pores capable of forming menisci and generating effective capillary tension under a given RH. This model reveals that shrinkage is regulated by two factors: the rate of RH decrease and the amount of effective pores that can participate in forming the capillary stress network (v_p).

$$\varepsilon_w = f\left(Ln(RH), v_p\right) \tag{1}$$

Experimental data indicate that the combined incorporation of SF and FA achieves efficient shrinkage suppression through the synergistic optimization of the aforementioned two factors. First, in terms of humidity regulation, as shown in Figures 5–8, under drying conditions, the SF-FA composite group exhibits the slowest initial rate of RH decline. This is because SF fills gel pores at the nanoscale, while FA fills capillary pores at the micron scale. This “dual-scale filling” effect not only reduces porosity but, more importantly, significantly refines the pore size gradation and reduces pore connectivity, thereby increasing transport resistance and creating a “throttling effect.” This effectively retards the decline in internal humidity, i.e. it reduces the decay rate of ln(RH) in Equation (1). Second, in terms of pore structure regulation, MIP results show that the microstructure formed by the SF-FA composite system exhibits a more uniform pore size distribution, along with a reduced proportion of gel pores and capillary pores. This implies that the composite system overall decreases the volume fraction of “effective pores” capable of generating capillary stress under a given RH. Consequently, the total net capillary stress generated per unit change in internal humidity is reduced, thereby achieving a “stress-relief effect”.

4. Conclusion

This study delved into the impact of mineral admixtures on the shrinkage deformation of shotcrete and delved into the underlying reasons for this influence from a microscopic viewpoint. The findings of this research lead to the following conclusions:

(1) When utilized independently or in conjunction, SF and FA demonstrate the ability to significantly improve the 28d compressive strength of shotcrete. This enhancement is primarily attributed to the micro-aggregate effect and pozzolanic reaction facilitated by these additives. Nevertheless, the sluggish hydration kinetics of FA render its standalone application less favorable for the early strength development of shotcrete.

(2) Mineral admixtures significantly inhibit the shrinkage deformation of shotcrete by reconstructing the microporous structure and regulating the hydration process. In the experiment, the development of the shrinkage deformation of shotcrete with age shows a two-stage pattern of "rapid growth stage in the early stage and decelerated development stage in the later stage". The rapid growth stage of shrinkage corresponds to the humidity saturation period, during which the shrinkage is mainly due to the chemical shrinkage of cement hydration. The decelerated development stage corresponds to the humidity attenuation period, and the shrinkage is mainly caused by self-drying. At the age of 28 days, the shrinkage rate of the group containing admixtures is lower than that of the control group. Among them, the SF-FA composite admixture group shows the best inhibitory effect - the shrinkage rate of the sealed specimens is 23.72% lower than that of the JZ group, and the shrinkage rate of the dry specimens is 17.76% lower. This reduction in shrinkage deformation is beneficial as it mitigates the negative impact on the durability and reliability of shotcrete.

(3) The shrinkage deformation of shotcrete is significantly influenced by its bubble characteristics and pore structure. Supplementary materials like SF and FA play a crucial role in enhancing the distribution of bubbles of varying sizes within the shotcrete matrix. The increased presence of numerous small bubbles helps mitigate the impact of capillary tension and surface tension on the solid-phase particles of shotcrete, providing a buffering effect within the material. Simultaneously, mineral admixtures synergistically regulate both the humidity field and the stress field. On one hand, the "dual-scale filling" by SF and FA optimizes the pore size distribution and connectivity, creating a "throttling effect" that significantly retards the rate of internal humidity decline. On the other hand, SF and FA also reduce the number of gel pores and capillary pores in shotcrete, decreasing the volume fraction of effective pores (v_p) which lowers the driving stress for shrinkage and produces a "stress-relief effect." The SF-FA composite system demonstrates the most pronounced synergistic optimization of the aforementioned two parameters, thus exhibiting the best performance in shrinkage inhibition.

References

Austin, S., & Robins, G. (1995). *Sprayed concrete: Principles and practice*. London: E & FN Spon.

British Standards Institution (2005). *BS EN 934-5:2005 Admixtures for concrete, mortar and grout*. London: British Standards Institution.

Bruce, M., Alexandre, B. P., Marc, J., & Benoit, B. (2022). Experimental study on the effect of key mix design parameters on shrinkage and cracking resistance of dry-mix shotcrete. *Construction and Building Materials*, *320*, 126216. doi: 10.1016/J.CONBUILDMAT.2021.126216.

Deng, G., He, Y. J., Lu, L. N., Wang, F. Z., & Hu, S. G. (2023). Pore structure evolution and sulfate attack of high-volume slag blended mortars under standard curing and steam curing. *Construction and Building Materials*, *363*, 129878. doi: 10.1016/J.CONBUILDMAT.2022.129878.

Garba, J. M., Tian, Y., Xie, Z. L., Yu, C. L., Hu, C. L., Chen, L., & Yuan, Q. (2024). Effect of accelerators on the long-term performance of shotcrete and its improvement strategies: A review. *Journal of Building Engineering*, *89*, 109364. doi: 10.1016/J.JOBE.2024.109364.

Han, Y. D., Zhang, J., Wang, J. H., & Hao, T. Y. (2017). Shrinkage control of concrete at early age based on coarse aggregate content. *Concrete*, *1*, 56–62. doi: CNKI:SUN:HLTF.0.2017-01-015.

Hang, M., Sun, Z., & Guo, Y. (2020). Experimental study on the shrinkage performance of concrete with different air contents. *Journal of Xi'an University of Architecture and Technology (Natural Science Edition)*, *52*(1), 15–20. doi: 10.15986/j.1006-7930.2020.01.003.

Hou, D. W. (2010). *Research on the integration of autogenous and drying shrinkage of concrete and related issues*. Beijing: Tsinghua University.

Huang, S. B. (2021). *Study on the influence of new alkali-free accelerator on concrete performance and pore structure*. Harbin: Harbin Institute of Technology. doi: 10.27061/d.cnki.ghgdu.2021.004142.

Li, X. (2013). Influence of mineral admixtures on early-age autogenous shrinkage of high-performance concrete. *Applied Mechanics and Materials*, *457-458*(457-458), 318–322. doi: 10.4028/WWW.SCIENTIFIC.NET/AMM.457-458.318.

Li, Y., Tan, M. H., Zhang, X., & Wu, K. R. (2000). Autogenous shrinkage of concrete and its research progress. *Journal of Building Materials*, *3*, 252–257. doi: CNKI:SUN:JZCX.0.2000-03-013.

Li, G. X., Zhang, J. B., Niu, M. D., & Song, Z. P. (2020). The mechanism of alkali-free liquid accelerator on the hydration of cement pastes. *Construction and Building Materials*, *233*, 117296. doi: 10.1016/j.conbuildmat.2019.117296.

Liu, J. Z., Sun, W., Miao, C. W., & Liu, J. P. (2009). Effect of mineral admixtures on drying shrinkage and autogenous shrinkage of low water-binder ratio concrete. *Journal of Southeast University (Natural Science Edition)*, *39*(3), 580–585. doi: CNKI:SUN:DNDX.0.2009-03-030.

Prudencio, L. R. (1998). Accelerating admixtures for shotcrete. *Cement and Concrete Composites*, *20* (2-3), 213–219. doi: 10.1016/S0958-9465(98)80007-3.

Qu, Z. Y., Yu, Q. L., Ji, Y. D., Gauvin, F., & Voets, I. K. (2020). Mitigating shrinkage of alkali activated slag with biofilm. *Cement and Concrete Research*, *138*, 106234. doi: 10.1016/j.cemconres.2020.106234.

Sheng, Y. P., Xue, B., Li, H. B., Qiao, Y., Chen, H. X., Fang, J. H., & Xu, A. H. (2017). Preparation and performance of a new-type alkali-free liquid accelerator for shotcrete. *Advances in Materials Science and Engineering*, *2017*, 1–9. doi: 10.1155/2017/1264590.

Singh, N., Kumar, P., & Goyal, P. (2019). Reviewing the behaviour of high volume fly ash based self compacting concrete. *Journal of Building Engineering*, *26*, 100882. doi: 10.1016/j.jobe.2019.100882.

Tang, Y., Xu, G. B., Lian, J., & Qu, C. L. (2016). Effect of temperature and humidity on the adhesion strength and damage mechanism of shotcrete-surrounded rock. *Construction and Building Materials*, *124*, 1109–1119. doi: 10.1016/j.conbuildmat.2016.08.126.

Wan, Z. M., He, T. S., Zheng, B., Qu, Q. H., Xue, R., & Xie, X. B. (2024). Influence of fly ash and granulated blast furnace slag on autogenous shrinkage and drying shrinkage of cement-based materials mixed with alkali accelerator and alkali-free accelerator. *Drying Technology*, *42*(14), 2137–2154. doi: 10.1080/07373937.2024.2407520.

Wang, J. H., Xie, Y. J., Zhong, X. H., & Li, L. J. (2020). Test and simulation of cement hydration degree for shotcrete with alkaline and alkali-free accelerators. *Cement and Concrete Composites*, *112*, 103684. doi: 10.1016/j.cemconcomp.2020.103684.

Wang, L. M., Zeng, L. P., Qiao, M., Wang, W., & Zhao, S. (2022a). Effect of low mineral admixtures on properties of C30 shotcrete. *Jiangsu Architecture*, *6*, 105–109. doi: CNKI:SUN:JSVF.0.2022-06-024.

Wang, L., He, X. X., Shu, C. X., Wei, Z. C., & Wang, H. (2022b). Research on the working performance and the corresponding mechanical strength of polyaluminum sulfate early strength alkali-free liquid accelerator matrix cement. *Materials*, *15*(22), 8086. doi: 10.3390/MA15228086.

Wang, J. H., Xie, Y. J., Zhong, X. H., & Qu, Y. A. (2022c). Humidity field in early-age shotcrete with alkaline and alkali-free accelerators. *Mechanics of Time-Dependent Materials*, *27*(2), 583–603. doi: 10.1007/S11043-022-09549-W.

Wang, J. H., Li, H. J., Tan, Y. B., Li, L. X., Qu, Y. A., & Xie, Y. J. (2023). Time-dependent autogenous shrinkage of shotcrete with alkaline and alkali-free accelerators. *Mechanics of Time-Dependent Materials*, *27*(2), 605–628. doi: 10.1007/S11043-023-09593-0.

Wu, L. M., Farzadnia, N., Shi, C. J., Zhang, Z. H., & Wang, H. (2017). Autogenous shrinkage of high performance concrete: A review. *Construction and Building Materials*, *149*, 62–75. doi: 10.1016/j.conbuildmat.2017.05.064.

Yang, R. H., He, T. S., & Xu, Y. D. (2022). Preparation of alkali free liquid accelerator for shotcrete with fluorosilicic acid waste liquid and its accelerating mechanism. *Cement and Concrete Composites*, *131*, 104600. doi: 10.1016/J.CEMCONCOMP.2022.104600.

Yuan, Q., Peng, M., & Li, Y. (2021). Review of the effects of high geothermal heat on the mechanical properties, pore structure, and hydration products of tunnel shotcrete. *Railway Engineering*, *61* (8), 53–58. doi: CNKI:SUN:TDJZ.0.2021-08-012.

Zhang, J., Hou, D. W., & Wei, S. (2010). Experimental study on the relationship between shrinkage and interior humidity of concrete at early age. *Magazine of Concrete Research*, *62*(3), 191–199. doi: 10.1680/macr.2010.62.3.191.

Zhang, J., Hou, D. W., & Han, Y. D. (2012). Micromechanical modeling on autogenous and drying shrinkages of concrete. *Construction and Building Materials*, *29*, 230–240. doi: 10.1016/j.conbuildmat.2011.09.022.

Zhang, Z., Zhang, B., & Yan, P. (2016). Hydration and microstructures of concrete containing raw or densified silica fume at different curing temperatures. *Construction and Building Materials*, *121*, 483–490. doi: 10.1016/j.conbuildmat.2016.06.014.

Corresponding author
Zhenbo Wang can be contacted at: wangzb@cumtb.edu.cn

Zhenbo Wang is a professor and doctoral supervisor at China University of Mining and Technology (Beijing), as well as the Director of the Development Center, School of Mechanics and Civil Engineering. He also serves as the Deputy Secretary - General of the Solid Waste and Eco - Materials Division of the Chinese Ceramic Society and the Vice Chair of the ECC Division of the China Concrete and Cement Products Association. Professor Wang has led over 20 national research projects. His research centers on performance - based optimization of engineered cementitious composites (ECC), solid - waste - derived cementitious materials, and concrete for marine engineering structures. He has received the Nomination Prize of the Chinese Ceramic Society Young Scientist Award and the First Prize of the Science and Technology Progress Award from the China Building Materials Federation. He has published more than 70 peer - reviewed papers, holds 7 granted Chinese invention patents and 2 utility model patents, and has participated in the drafting of 7 industry standards in the building materials sector.